

## Evidence that ganglioside enriched domains are distinct from caveolae in MDCK II and human fibroblast cells in culture

Vanna Chigorno<sup>1</sup>, Paola Palestini<sup>2</sup>, Mariateresa Sciannamblo<sup>1</sup>, Vincenza Dolo<sup>3</sup>, Antonio Pavan<sup>3</sup>, Guido Tettamanti<sup>1</sup> and Sandro Sonnino<sup>1</sup>

<sup>1</sup>Study Center for the Functional Biochemistry of Brain Lipids, Department of Medical Chemistry and Biochemistry – LITA-Segrate, University of Milan, Italy; <sup>2</sup>Department of Experimental, Environmental and Biotechnological Medicine, University of Milano Bicocca, Monza, Italy; <sup>3</sup>Department of Experimental Medicine, University of L'Aquila, Italy

Cultures of MDCK II and human fibroblast cells were fed radioactive sphingosine and a radioactive GM3 ganglioside derivative containing a photoactivable group. The derived cell homogenates were treated with Triton X-100 and fractionated by sucrose-gradient centrifugation to prepare a detergent-insoluble membrane fraction known to be enriched in sphingolipid and caveolin-1, i.e. of caveolae.

The detergent-insoluble membrane fraction prepared after feeding [ $1\text{-}^3\text{H}$ ]sphingosine to cells, was found to be highly enriched, with respect to protein content, in metabolically radiolabeled sphingomyelin and glycosphingolipids (about 18-fold). By feeding cells photoactivable radioactive GM3, after 2 h-chase, caveolin-1, CAV1, and proteins of high molecular mass became cross-linked to GM3, the cross-linking complexes being highly concentrated in the detergent-insoluble membrane fraction. The interaction between the ganglioside derivative and CAV1 was a time-dependent, transient process so that CAV1 cross-linking to GM3 was hardly detectable after a 24-h chase followed the pulse time. After a 24-h chase, only the high molecular mass proteins cross-linked to GM3 could be clearly observed. These results suggest that a portion of the GM3 administered to cells enters caveolae and moves to the glycosphingolipid domains, or enters caveolae that are then rapidly catabolized.

Electron microscopy of cells in a culture immunostained with a monoclonal antibody to GM3 and a secondary gold-conjugated antibody detected several clusters of gangliosides on the plasma membranes separate from caveolae; gangliosides located inside the caveolae could not be detected. Scanning confocal microscopy of cells immunostained with anti-GM3 and anti-CAV1 Ig showed only a very small overlap with the CAV1 and GM3 signals.

Thus, the biochemical and microscopic studies suggest that caveolae contain at most a low level of gangliosides and are separate from the GM3 ganglioside enriched domains.

**Keywords:** gangliosides; GM3; sphingolipid domains; caveolin-1; caveolae.

In recent years, particular attention has been paid to cell membrane domains with peculiar lipid/protein compositions, i.e. to restricted membrane areas where the concentration and, or, nature of components is different than in the remainder membrane environment [1–5]. Owing to the improvement of fractionation techniques for the isolation of membrane domains [3–5], information on the composition of these domains has grown rapidly. In particular, domains that are enriched in gangliosides, sphingomyelin, cholesterol, receptor and non-receptor tyrosine kinases, heterotrimeric G proteins and G

protein-coupled receptors, integral membrane proteins and porin have been characterized [6,7].

Gangliosides, sialic-acid-containing glycosphingolipids, are components of the outer lipid layer of cell plasma membranes. At the water/lipid interface, the individual ganglioside molecules occupy a large surface area due to their bulky oligosaccharide chain [8]. The presence of such a large hydrophilic moiety in the ganglioside structure, together with the possibility of forming a net of intermolecular hydrogen bonds *via* the amide group of sphingolipid sphingosine at the

Correspondence to S. Sonnino, Dipartimento di Chimica e Biochimica Medica – LITA-Segrate, Via Fratelli Cervi 93, 20090 Segrate (Milano), Italy.

Fax: + 390226423209, E-mail: Sandro.Sonnino@unimi.it

**Abbreviations:** GM3,  $\text{II}^3\text{-}\alpha\text{-Neu5AcLacCer}$ ,  $\alpha\text{-Neu5Ac-(2-3)-}\beta\text{-Gal-(1-4)-}\beta\text{-Glc-(1-1)-Cer}$ ; [ $11\text{-}^3\text{H}(\text{Neu5Ac})$ ]GM3,  $\alpha\text{-Neu5}[^3\text{H}]\text{Ac-(2-3)-}\beta\text{-Gal-(1-4)-}\beta\text{-Glc-(1-1)-Cer}$ ; [ $11\text{-}^3\text{H}(\text{Neu5Ac})$ ]GM3- $\text{N}_3$ ,  $\alpha\text{-Neu5}[^3\text{H}]\text{Ac-(2-3)-}\beta\text{-Gal-(1-4)-}\beta\text{-Glc-(1-1)-}\{(2\text{S},3\text{R},4\text{E})\text{-2-[12-(2-nitro-4-azidophenyl)amino-dodecanoyl]amino-3-hydroxy-octadec-4-ene}\}$ ; GM1,  $\text{II}^3\text{-}\alpha\text{-Neu5AcGg}_4\text{Cer}$ ,  $\beta\text{-Gal-(1-3)-}\beta\text{-GalNAc-(1-4)-}[\alpha\text{-Neu5Ac-(2-3)-}]\beta\text{-Gal-(1-4)-}\beta\text{-Glc-(1-1)-Cer}$ ; [ $11\text{-}^3\text{H}(\text{Neu5Ac})$ ]GM1- $\text{N}_3$ ,  $\beta\text{-Gal-(1-3)-}\beta\text{-GalNAc-(1-4)-}[\alpha\text{-Neu5}[^3\text{H}]\text{Ac-(2-3)-}]\beta\text{-Gal-(1-4)-}\beta\text{-Glc-(1-1)-}\{(2\text{S},3\text{R},4\text{E})\text{-2-[12-(2-nitro-4-azidophenyl)amino-dodecanoyl]amino-3-hydroxy-octadec-4-ene}\}$ ; LacCer,  $\beta\text{-Gal-(1-4)-}\beta\text{-Glc-(1-1)-Cer}$ ; GlcCer,  $\beta\text{-Glc-(1-1)-Cer}$ ; Cer, ceramide (2S,3R,4E)-2-(octadecanoyl)amino-1,3-dihydroxy-octadec-4-ene; sphingosine,  $\text{C}_{18}$ -sphingosine (2S,3R,4E)-2-amino-1,3-dihydroxy-octadec-4-ene; [ $1\text{-}^3\text{H}$ ]sphingosine, (2S,3R,4E)-2-amino-1,3-dihydroxy-[ $1\text{-}^3\text{H}$ ]octadec-4-ene; Neu5Ac, N-acetylneuraminic acid; EMEM, Eagle's minimum essential medium; CLAP, a mixture of chymostatin, leptin, antipain and pepstatin; CAV1, caveolin-1; FITC, fluorescein isothiocyanate.

**Note:** ganglioside nomenclature is according to Svennerholm, L. (1980) *Adv. Exp. Biol. Med.* **125**, 11 and the IUPAC-IUBMB recommendations (1998)

*Pure Appl. Chem.* **69**, 2475–2487 and *Carbohydr. Res.* **312**, 167–175.

(Received 10 March 2000, revised 8 May 2000, accepted 9 May 2000)

water/lipid interface, should promote the formation of rigid sphingolipid enriched domains [9–11]. Interactions between gangliosides and proteins [12], such as those between GM3 and c-Src, Rho, FAK and Ras [13,14] or between GD3 and Lyn [15], specifically occur in the ganglioside enriched membrane domains and may be instrumental for the process of transmembrane signaling [16].

A particular type of domain, both morphologically and compositionally characterized, consists of caveolae, flask-shaped invaginations of the plasma membrane, lacking clathrin coating, and characteristically enriched in caveolin-1 (CAV1), a 21- to 24-kDa integral membrane protein [17,18].

In this paper, we report a study performed with a combination of different experimental approaches aimed to obtain information on ganglioside-enriched domains in cultured MDCK II and fibroblast cells, where GM3 is the main ganglioside: feeding isotopically tritium labeled sphingosine to cells was performed to metabolically label sphingolipids; this was followed by characterization of the sphingolipid-enriched domains. Photolabeling experiments with a photoactivable radioactive derivative of GM3 were performed to follow the interaction processes occurring between gangliosides and CAV1 and to have information on the presence of GM3 in the caveolae and microscopical studies were performed to identify clusters of gangliosides at the cell surface.

## MATERIALS AND METHODS

### Materials

The commercial chemicals were the purest available, common solvents were distilled before use and deionized water, obtained by a MilliQ system (Millipore, Bedford, MA, USA), was distilled in a glass apparatus. High performance silica gel precoated thin-layer plates (HPTLC Kieselgel 60, 10 × 10 cm) were purchased from Merck GmbH (Darmstadt, Germany); sodium boro[<sup>3</sup>H]hydride (8 Ci·mmol<sup>-1</sup>) and [<sup>3</sup>H]acetic anhydride (4.6 Ci·mmol<sup>-1</sup> and 7 Ci·mmol<sup>-1</sup>) from Amersham International (Bucks, UK); rabbit polyclonal anti-(CAV1) Ig sc-894 and protein G-Sepharose beads were from Santa Cruz Biotechnology Inc. (Santa Cruz, CA, USA); polyclonal anti-caveolin Ig C13630 from Transduction Laboratories (Lexington, KY, USA); anti-GM3 mAb was provided by T. Tai (Department of Tumor Immunology, Metropolitan Institute of Medical Science, Tokyo); colloidal gold-conjugated protein A was from Pharmacia Fine Chemicals (Uppsala, Sweden); *Vibrio cholerae* sialidase, *Bacillus cereus* sphingomyelinase, rabbit anti-(mouse IgM) Ig, HRP-conjugated mouse anti-(rabbit IgG) Ig, trypsin, bovine serum albumin, tricine buffer, CLAP (chymostatin, leupeptin, antipain and pepstatin) and aprotinin were from Sigma (St Louis, MO, USA); poly(vinylidene difluoride) membranes for Western blotting were from Millipore (Bedford, MA, USA); *Macrobdella decora* ceramide glycanase was from Boehringer Mannheim (Mannheim, Germany). Ganglioside GM3 was prepared from bovine brain GM1 as described in [19] and sphingosine from cerebroside as described in [20]. MDCK II cells were kindly provided by K. Simons (EMBL, Heidelberg, Germany).

### Preparation of radioactive gangliosides, sphingosine and standard compounds

Isotopically labeled GM3 containing tritium at position 11 of sialic acid, [11-<sup>3</sup>H(*Neu5Ac*)]GM3 (homogeneity over 99%; specific radioactivity, 2.3 Ci·mmol<sup>-1</sup>), was prepared by

deacetylation of GM3 followed by N-acetylation with [<sup>3</sup>H]acetic anhydride [21,22].

The GM3 derivative tritium-labeled at position 11 of sialic acid and containing an azide group in the modified acyl chain, [11-<sup>3</sup>H(*Neu5Ac*)]GM3-N<sub>3</sub> (homogeneity over 99%; specific radioactivity, 3.5 Ci·mmol<sup>-1</sup>), was prepared, for the first time, from natural GM3 according to the scheme of reactions shown in Fig. 1, previously developed for the synthesis of [11-<sup>3</sup>H(*Neu5Ac*)]GM1-N<sub>3</sub> [23].

[1-<sup>3</sup>H]Sphingosine (homogeneity over 98%; specific radioactivity of 2 Ci·mmol<sup>-1</sup>) was prepared by specific chemical oxidation of the primary hydroxyl group of sphingosine followed by reduction with sodium boro[<sup>3</sup>H]hydride [24].

<sup>3</sup>H-Labeled ceramide, sphingomyelin, phosphatidylethanolamine, lactosylceramide and ganglioside GD3 were extracted from [1-<sup>3</sup>H]sphingosine-fed cells (see below), purified, characterized and used as chromatographic standards.

### Cell cultures

MDCK II cells were cultured to 80–90% confluence and human skin fibroblasts to confluence, as previously described [25,26].

### Treatment of cell cultures with [1-<sup>3</sup>H]sphingosine, [11-<sup>3</sup>H(*Neu5Ac*)]GM3 and [11-<sup>3</sup>H(*Neu5Ac*)]GM3-N<sub>3</sub>

[1-<sup>3</sup>H]Sphingosine, [11-<sup>3</sup>H(*Neu5Ac*)]GM3, a mixture of [11-<sup>3</sup>H(*Neu5Ac*)]GM3-N<sub>3</sub> and nonradioactive natural GM3 (1 : 10, mol/mol; this dilution with cold GM3 is necessary to reduce self quencing during illumination), were separately dissolved in methanol, pipetted into a sterile tube and dried under a nitrogen stream. Each residue was solubilized in an appropriate volume of prewarmed (37 °C) Eagle's minimal essential medium (EMEM), in the presence of 2% fetal bovine serum to obtain a sphingosine concentration of 3 × 10<sup>-8</sup> M, or, in the absence of fetal bovine serum, to obtain a ganglioside concentration ranging from 5 × 10<sup>-7</sup> M to 2.5 × 10<sup>-5</sup> M. After removal of the original medium and rapid washing of cells with EMEM, 5 mL of the medium containing the radioactive lipid was added to each 100-mm dish and the cells were incubated (pulse time) at 37 °C. The pulse with radioactive sphingosine was of 2 h and that with gangliosides of 4 h. After incubation, the radioactive medium was removed and the dishes were washed, first with EMEM solution (for 5 min), then (for 30 min) with 10% fetal bovine serum/EMEM. Chase time was 48 h after feeding [1-<sup>3</sup>H]sphingosine, 2 and 24 h after feeding [11-<sup>3</sup>H(*Neu5Ac*)]GM3 and [11-<sup>3</sup>H(*Neu5Ac*)]GM3-N<sub>3</sub>. After chase, cells were washed twice with NaCl/P<sub>i</sub> and once with the appropriate solution for the subsequent processing. Treatments with [11-<sup>3</sup>H(*Neu5Ac*)]GM3-N<sub>3</sub> were performed in the dark and photolabeling activated by a 30-min illumination on ice with an UV lamp at 366 nm.

Treated cells were scraped off with a rubber policeman, centrifuged at 1000 g for 10 min and subjected to lipid and protein analyses or membrane fraction preparations.

### Preparation of plasma membranes and detergent-insoluble membrane fraction

The preparation of plasma membrane subcellular fractions and detergent-insoluble membrane fractions was carried out according to described procedures [3,4,27]. Purified plasma membranes were prepared and used in some experiments to

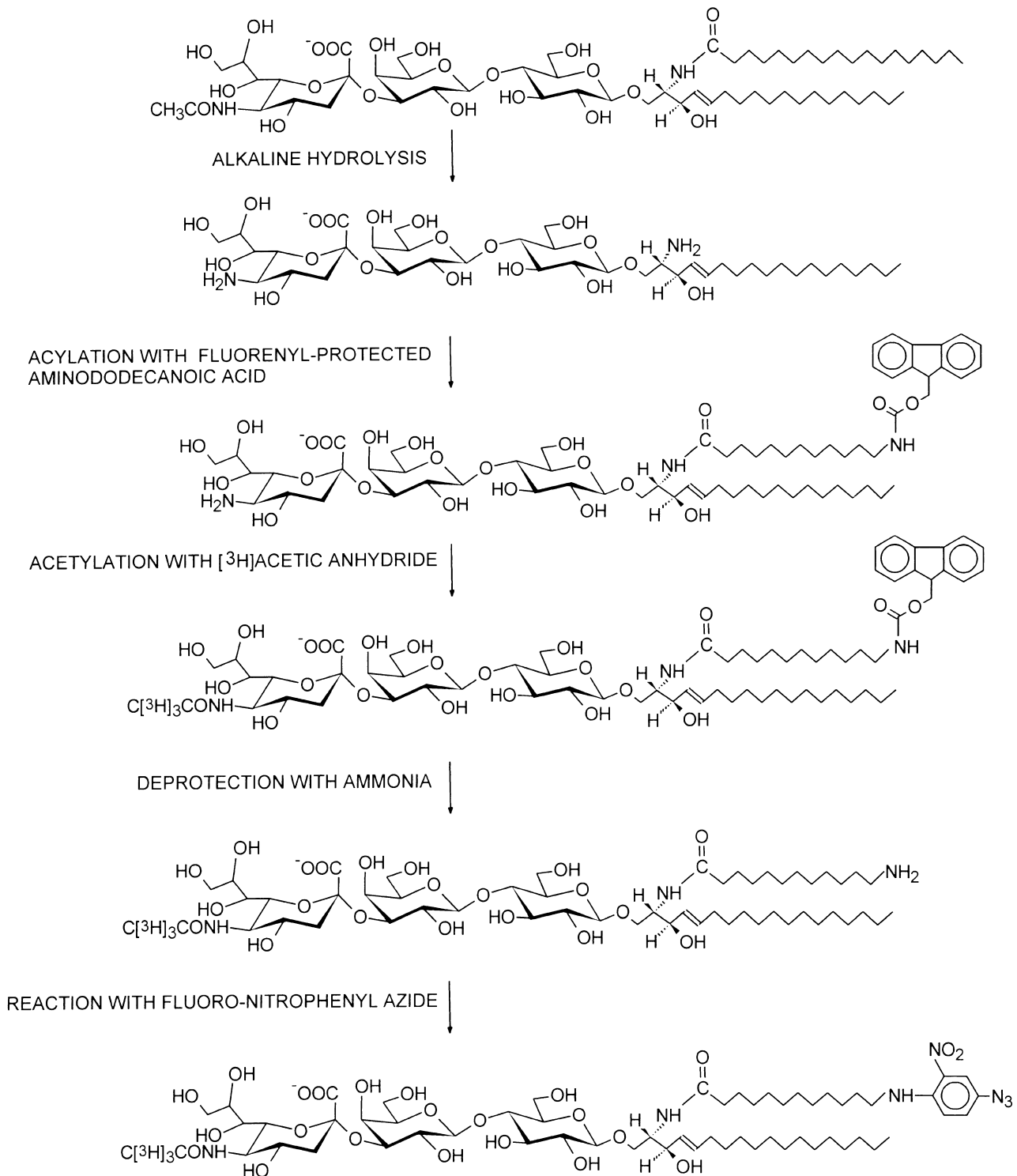


**Fig. 1.** Scheme of the reactions for the preparation of radioactive and photoactivable GM3, [<sup>11-<sup>3</sup>H(Neu5Ac)]GM3-N<sub>3</sub>, from natural GM3. Reaction chemical conditions were those reported for the synthesis of [<sup>11-<sup>3</sup>H(Neu5Ac)]GMI-N<sub>3</sub> [28].</sup></sup>

study plasma membrane proteins cross linked to GM3 by photolabeling experiments. The detergent-insoluble membrane fraction is prepared by sucrose gradient fractionation of a postnuclear cell fraction. All the gradient fractions were analysed for sphingolipid content and enrichment. The detergent-insoluble membrane fraction is known to be highly enriched, with respect to its protein content, of sphingolipids [4] and CAV1 [28].

#### Cell lipid extraction and characterization

The different cell-derived preparations were subjected to lipid extraction [29], resulting in a delipidized pellet and a total lipid mixture. Lipids were analysed by TLC, in comparison with standard compounds, followed by radioactivity imaging (see below). The main radioactive lipids were purified by the TLC blotting technique [30] and characterized by enzymatic and

chemical treatments. In particular, gangliosides GM3 and GD3 dissolved in 50  $\mu\text{L}$  water, were treated at 37 °C for 2 h with 1 mU of *V. cholerae* sialidase, to yield lactosylceramide, and both GM3 and lactosylceramide, respectively; the same GM3 and GD3, dissolved in 500  $\mu\text{L}$  of 25 mM acetate buffer, pH 5, 0.075% sodium cholate, were treated at 37 °C for 18 h with 1 mU of *M. decora* ceramide glycanase, to yield ceramide. Sphingomyelin, dissolved in 30  $\mu\text{L}$  of 100 mM Tris/HCl, pH 7.4, 0.5 mM  $\text{MgCl}_2$ , 0.05% sodium deoxycholate, was treated at 37 °C overnight with 11 mU of *B. cereus* sphingomyelinase, to yield ceramide. Phosphatidylethanolamine, formed by recycling of the radioactive ethanolamine produced in the catabolism of sphingosine [31], was characterized following its degradation under alkaline conditions. The reaction mixtures were separated by TLC (see below) and the reaction products identified by chromatographic comparison with standard lipids.

### PAGE and Western-blotting analyses

The protein patterns in the cell homogenate, plasma membranes and detergent-insoluble membrane fraction were analyzed by SDS/PAGE and Western blotting. SDS/PAGE was carried out as described previously [18] using 12% polyacrylamide gel. 2D electrophoretic separation was performed with the BioRad Mini-protean II 2D system according to the manufacturer's recommendations; a 15% polyacrylamide gel was used for the second dimension. Western blotting was performed as reported previously [32] with minor modifications. The gel was soaked in the transfer buffer (10 mM Caps, pH 11, in 10% methanolic solution) for 5 min, sandwiched with a poly(vinylidene difluoride) membrane and transferred for 2 h at 200 mA at 4 °C. The poly(vinylidene difluoride) membrane was blocked overnight at 4 °C, with 1% BSA, 1% nonfat dry milk, in 10 mM Tris/HCl, pH 8, 150 mM NaCl, and incubated for 2 h at room temperature with rabbit anti-CAV1 IgG (1  $\mu\text{g}\cdot\text{mL}^{-1}$ ) in the blocking solution, containing 0.05% Tween-20. After four washes with the blocking solution, the poly(vinylidene difluoride) membrane was incubated for 2 h at room temperature with mouse anti-(rabbit IgG) Ig, diluted 1 : 3000 with the blocking solution. Caveolin-1 was detected with the ECL method according to the manufacturer's instructions (Amersham). When homogenates and membrane fractions were analysed by SDS/PAGE, the radioactive lipids migrated at the electrophoretic front. Preliminary experiments showed that only a minor part of radioactive GM3 cross-linked lipids could be transferred to the poly(vinylidene difluoride) membranes under optimal conditions for protein Western-blotting analysis.

### Immunoprecipitation with anti-CAV1

Immunoprecipitation with anti-CAV1 Ig sc-894 and C13630 was carried out as described [27], with minor modifications. Briefly, cell homogenate and membrane fraction were lysed at 37 °C for 20 min with 500  $\mu\text{L}$  of 25 mM Tris/HCl, pH 7.4, 150 mM NaCl, 1% Triton X-100, and 0.1% CLAP. The suspension was mixed with 30  $\mu\text{L}$  of protein G–Sepharose beads and incubated for 2 h at 4 °C to preclude nonspecific binding. After centrifugation (1 min at 270 g), the lysate was incubated overnight at 4 °C with rabbit anti-caveolin Ig. After addition of 30  $\mu\text{L}$  of protein G–Sepharose beads, incubation was continued for 2 h at 4 °C. Beads were then washed and proteins detached with the Laemmli buffer by heating for 10 min at 100 °C.

### Determination of sphingolipid enrichment

The specific enrichment of sphingolipids in the different fractions has been referred to the protein content, i.e.:

$$\text{Enrichment} = \left( \frac{\text{d.p.m. in fraction}}{\text{d.p.m. in homogenate}} \right) \times \left( \frac{\mu\text{g protein in homogenate}}{\mu\text{g protein in fraction}} \right)$$

### Electron microscopy

For detection of ganglioside GM3 distribution over the cell plasma membrane, MDCK II cells were harvested, washed, fixed with 2% formaldehyde and incubated with anti-GM3 Ig (20  $\mu\text{g}\cdot\text{mL}^{-1}$  in NaCl/ $\text{P}_i$  with 0.03% BSA) for 1 h. The cells were then washed three times with NaCl/ $\text{P}_i$  containing 0.03% BSA and incubated with rabbit anti-(mouse IgM) Ig (1 : 10 in NaCl/ $\text{P}_i$ , for 1 h at 4 °C) and then fixed with glutaraldehyde (1% in NaCl/ $\text{P}_i$  for 1 h at 4 °C). After extensive washing in NaCl/ $\text{P}_i$ , cells were labeled with colloidal gold-conjugated protein A. In separate and parallel experiments, cells were fixed with glutaraldehyde (1% in NaCl/ $\text{P}_i$  for 1 h at 4 °C) immediately after the incubation with anti-GM3 mAb and before the secondary anti-(mouse IgM) Ig, as reported previously [33]. After washing, the cells were fixed with 2% glutaraldehyde, postfixed with 1%  $\text{OsO}_4$ , dehydrated with ethanol, infiltrated with acetone, and embedded in Epon. Ultrathin sections were poststained with uranyl acetate and lead

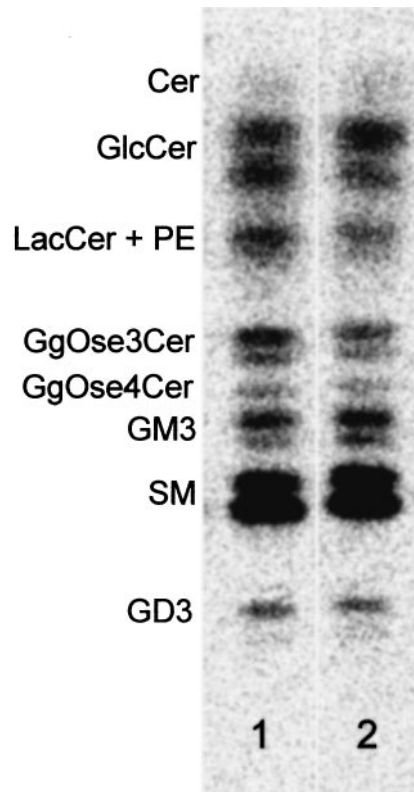


Fig. 2. TLC separation of the total lipid extract from human fibroblast cells fed [ $^3\text{H}$ ]sphingosine. Lane 1, lipids from homogenates; lane 2, lipids from the detergent-insoluble membrane fraction. Solvent system, chloroform/methanol/0.2% aqueous  $\text{CaCl}_2$ , 55 : 45 : 10, v/v. Detection by radioactivity imaging; acquisition time, 24 h.

citrate, and examined under an electron microscope (Philips CM100).

### Scanning confocal microscopy

MDCK II cells, grown on coverslip, were fixed with 2% formaldehyde in NaCl/P<sub>i</sub> for 30 min. After washing, cells were incubated in blocking solution for 30 min. Anti-GM3 Ig was added for 1 h, then, after three washes in NaCl/P<sub>i</sub>, the cells were incubated with fluorescein isothiocyanate (FITC)-conjugated goat anti-(mouse IgG) Ig for 1 h. After washing, permeabilization was carried out with 0.5% Triton X-100 in NaCl/P<sub>i</sub> for 15 min. After three washes, anti-CAV1 Ig was added for 1 h, and subsequently Texas Red-conjugated goat anti-(rabbit IgG) Ig was added for 1 h. Cells were finally washed three times in NaCl/P<sub>i</sub> and then mounted upside-down onto a glass slide in glycerol/water (9 : 1, v/v) and analysed by scanning confocal microscopy in dual fluorescence configuration where the FITC (green) and the Texas Red (red) fluorophores were excited at 518 and 488 nm, respectively. Images were acquired through a confocal laser scanning

microscope Sarastro 000 (Molecular Dynamics) adapted to a Nikon Optiphot microscope (objective PLAN-APO 60/1.4 oil) and equipped with argon ion laser set at a power of 1 mW. Images were collected at 512 × 512 pixels with voxel dimensions 0.08 mm (lateral), 0.49 mm (axial). After having been processed with routines for noise filtering, serial optical sections were assembled in a depth-coding mode. Acquisition and processing were carried out using IMAGE SPACE software (Molecular Dynamics).

### Other analytical methods

TLC was performed with the solvent system chloroform/methanol/0.2% aqueous CaCl<sub>2</sub>, 50 : 42 : 11 (v/v), to assess the homogeneity of radioactive GM3 and to analyse the enzymatic reaction mixtures, and with chloroform/methanol/water, 55 : 45 : 10 (v/v), to assess the total lipid mixture compositions.

The radioactivity associated with total homogenates, membrane fractions, total lipid extracts and delipidized pellets, was determined by liquid scintillation counting. Radioactivity

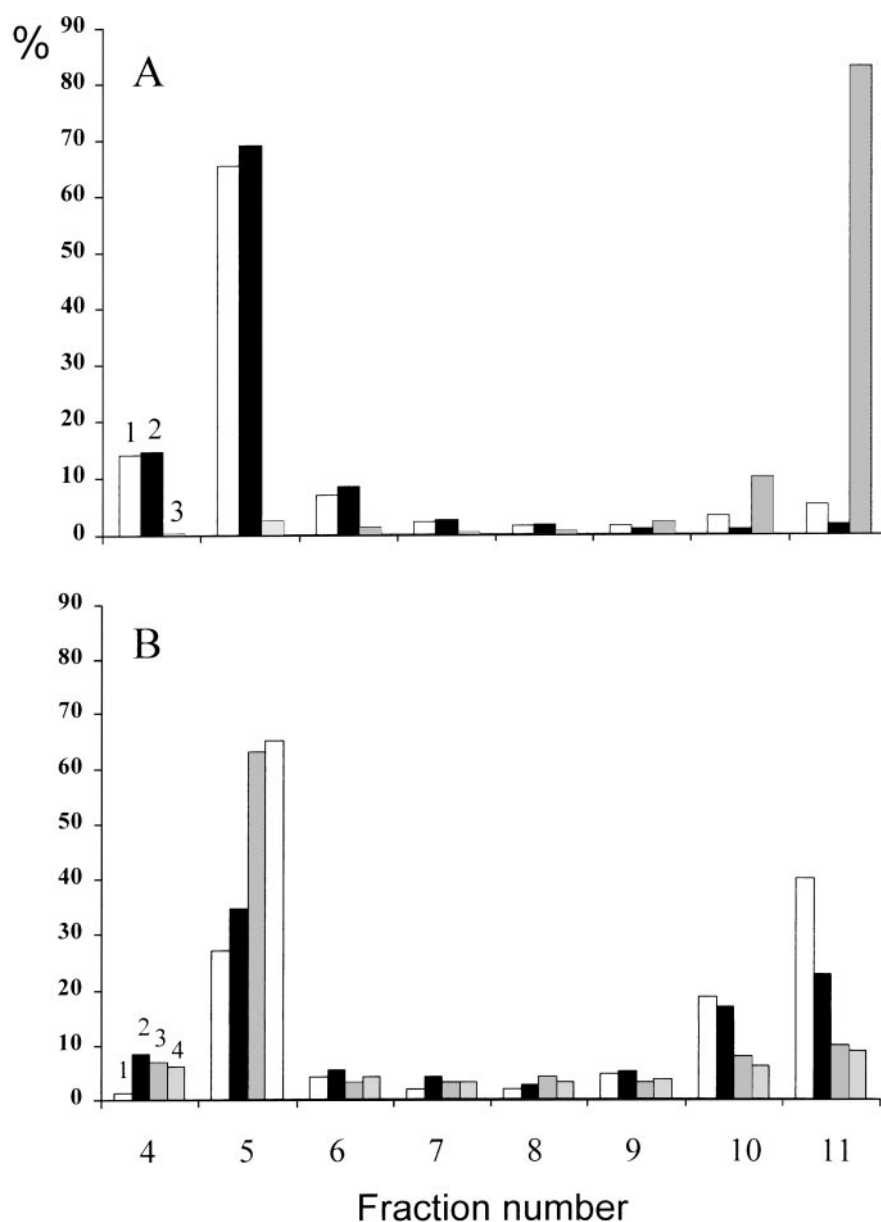


**Fig. 3. Sucrose-gradient fractionation of a postnuclear fraction prepared from detergent treated fibroblast cell homogenate.** Fraction 1 was collected at the top of the gradient and the pellet containing fraction 11 was at the bottom. Fraction 5 contained the light scattering band located between 5 and 30% sucrose. Fractions 1–3 did not contain radioactivity or proteins. (A) Distribution of sphingolipid radioactivity and protein content in sucrose gradient fractions from cells fed [<sup>3</sup>H]sphingosine: [<sup>3</sup>H]GM3, bars 1; [<sup>3</sup>H]SM, bars 2; protein, bars 3. (B) Distribution of sphingolipid radioactivity in sucrose gradient fractions from cells fed [<sup>11</sup>-<sup>3</sup>H(*Neu5Ac*)]GM3-N<sub>3</sub> followed by: 2-h chase, bars 1; from cells fed [<sup>11</sup>-<sup>3</sup>H(*Neu5Ac*)]GM3-N<sub>3</sub> followed by 24-h chase, bars 2, from cells fed [<sup>11</sup>-<sup>3</sup>H(*Neu5Ac*)]GM3 followed by 2-h chase, bars 3, and from cells fed [<sup>11</sup>-<sup>3</sup>H(*Neu5Ac*)]GM3 followed by 24-h chase, bars 4.

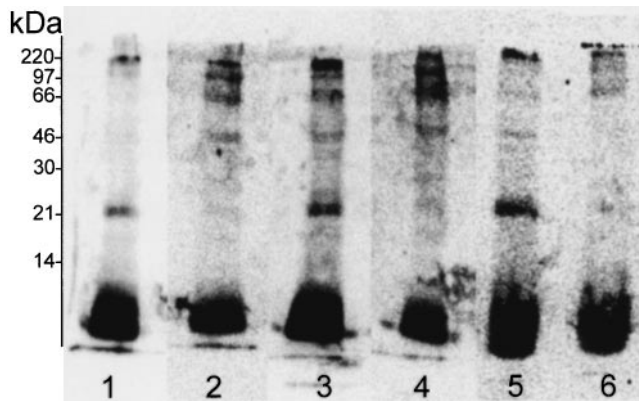


Fig. 4. SDS/PAGE of the homogenates from MDCK II and human fibroblast cells fed  $[11\text{-}^3\text{H}(\text{Neu5Ac})]\text{GM3-N}_3$  and illuminated. Lane 1, MDCK II cells subjected to 2-h chase; lane 2, MDCK II cells subjected to 24-h chase; lane 3, human fibroblasts subjected to 2-h chase; lane 4, human fibroblasts subjected to 24-h chase; lane 5, sphingolipid enriched domains prepared from human fibroblasts subjected to 2-h chase; lane 6, sphingolipid enriched domains prepared from human fibroblasts subjected to 24-h chase. The darkest bands at the front of the gel are the radioactive lipids. Detection by radioactivity imaging; acquisition time, 73 h.

imaging of TLC plates, SDS-PAGE and of poly(vinylidene difluoride) membranes was acquired with a  $\beta$ -imager 2000 instrument (Biospace, Paris). The radioactivity associated with individual lipids and proteins was determined with the specific  $\beta$ -VISION software provided by the manufacturer (Biospace).

Structural characterization of sphingosine, GM3 and intermediates of the synthesis of radioactive and photoactivable GM3 was carried out by high resolution NMR spectroscopy [34]

The protein content was determined according to Lowry *et al.* [35], by the micro BCA kit (Pierce), and as dot spot revealed by Coomassie blue staining, using bovine serum albumin in the presence of sucrose, as the reference standard.

## RESULTS

### Experiments with $[1\text{-}^3\text{H}]\text{sphingosine}$

Fibroblasts feeding with  $[1\text{-}^3\text{H}]\text{sphingosine}$  was carried out to study the sphingolipid enrichment, with respect to the protein content, in the detergent-insoluble (sphingolipid-enriched) membrane fraction.

$[1\text{-}^3\text{H}]\text{sphingosine}$  was taken up by fibroblasts very quickly, and entered, as expected [31,36] the biosynthetic pathway of sphingolipids. In addition to sphingolipids, phosphatidylethanolamine became radioactive owing to recycling of the radioactive ethanolamine that derived from the portion of sphingosine undergoing degradation. The radioactive lipid pattern, sphingolipids and phosphatidylethanolamine, of fibroblast homogenate and detergent-insoluble membrane fraction prepared from fibroblasts, as determined by TLC and radioactivity imaging, is reported in Fig. 2, lanes 1 and 2, respectively. In the detergent-insoluble membrane fraction the sphingolipid radioactivity distribution was similar to that found in the homogenate. Figure 3A shows that the detergent-insoluble membrane fraction is highly enriched in sphingolipids, gangliosides (bar 1) and sphingomyelin (bar 2). The majority of cell proteins (bar 3) were located in the heavier fractions located at the bottom of sucrose gradient, while the

detergent-insoluble membrane fraction corresponding to fraction 5 contained only 2–3% of the total cell protein. From five different experiments, the sphingolipid enrichment, referred to homogenate proteins, was  $18 \pm 4$ -fold in the detergent-insoluble membrane fraction. The detergent-insoluble membrane fraction was, as expected [28], also enriched in CAV1 protein (data not shown).

### Photolabeling experiments with $[11\text{-}^3\text{H}(\text{Neu5Ac})]\text{GM3-N}_3$

MDCK II and fibroblasts cells were fed  $[11\text{-}^3\text{H}(\text{Neu5Ac})]\text{GM3-N}_3$  for 4 h in the absence of fetal bovine serum. Then, the medium containing the ganglioside derivative was removed and the cells were carefully washed to remove loosely bound gangliosides [37], and maintained in culture (chase) for 2 h or 24 h in the presence of fetal bovine serum and illuminated. The radioactivity associated with proteins by cross-linking with the radioactive GM3 derivative was studied in the total cell homogenate, in a plasma-membrane-enriched fraction or in a detergent-insoluble membrane fraction.

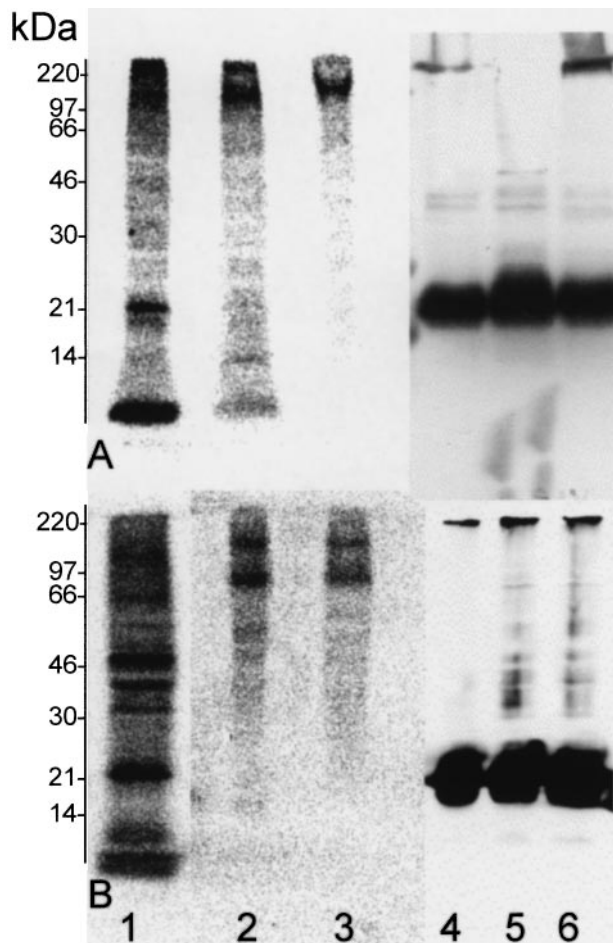


Fig. 5. Western-blotting analysis of the homogenates from MDCK II and human fibroblast cells fed  $[11\text{-}^3\text{H}(\text{Neu5Ac})]\text{GM3-N}_3$  or  $[11\text{-}^3\text{H}(\text{Neu5Ac})]\text{GM3}$ . (A) MDCK II cells; (B) human fibroblast cells. Lanes 1, 2 and 3, detection by radioactivity imaging; acquisition, 72 h; lanes 4, 5 and 6, immunoblotting with anti-CAV1 Ig and detection by ECL method; exposure time, 5 min. Lanes 1 and 4, cells fed  $[11\text{-}^3\text{H}(\text{Neu5Ac})]\text{GM3-N}_3$  and subjected to 2-h chase followed by illumination; lanes 2 and 5, cells fed  $[11\text{-}^3\text{H}(\text{Neu5Ac})]\text{GM3-N}_3$  and subjected to 24-h chase followed illumination; lanes 3 and 6, cells fed  $[11\text{-}^3\text{H}(\text{Neu5Ac})]\text{GM3}$  and subjected to 24-h chase.

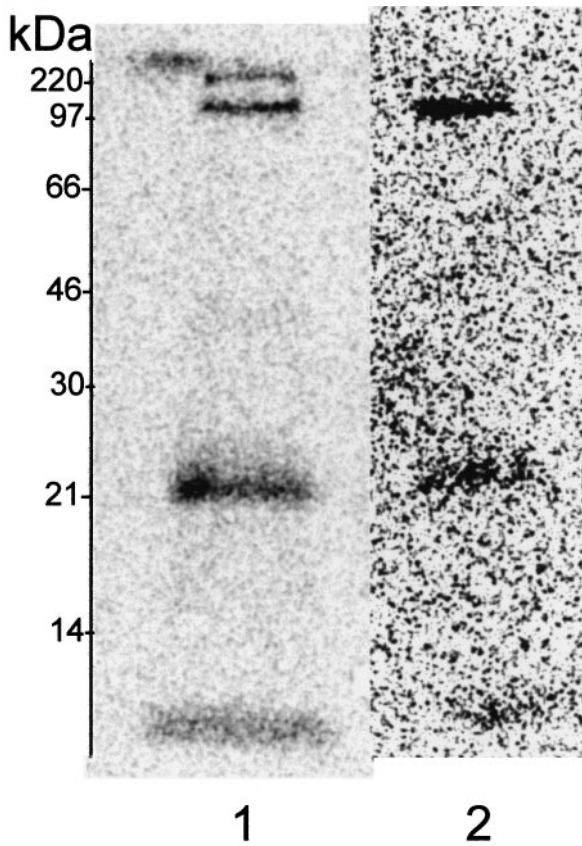


Fig. 6. SDS/PAGE of immunoprecipitates with anti-CAV1 antibody from the homogenate from human fibroblast cells fed  $[11\text{-}^3\text{H}(\text{Neu5Ac})]\text{GM3-N}_3$ . Detection by radioactivity imaging. Acquisition time, 73 h; lane 2 has been enhanced by software. Lane 1, cells subjected to 2-h chase; lane 2, cells subjected to 24-h chase.

After a 2-h chase, the cell radioactivity associated with lipids was about 90%, and that associated with proteins about 10% (Fig. 4, lanes 1 and 3). After 24 h the two values became about 75% and 25%, respectively (Fig. 4, lanes 2 and 4).

After a 2-h chase followed by illumination, a radioactive protein with an apparent molecular mass of about 20- to 25-kDa and behavior similar to that of CAV1 (Fig. 5) was one of the major radioactive proteins, about 50% of the total radioactive proteins, in both MDCK II and fibroblast cell lines. In some experiments, cells were treated with trypsin before illumination in order to remove the radioactive ganglioside derivative bound to cell surface proteins [37]. No differences in radioactivity intensity of the 20- to 25-kDa band was observed between trypsin-treated and untreated cells, suggesting that the 20- to 25-kDa protein is not be exposed at the cell surface. After 24-h chase, in both the MDCK II and fibroblast cell lines, the amount of the 20- to 25-kDa protein cross-linked to GM3 was very low (Fig. 5). SDS/PAGE of the immunoprecipitate obtained by immunoprecipitation of the fibroblast homogenate with polyclonal anti-caveolin Ig showed a radioactive band of 20- to 25-kDa (Fig. 6). Figure 7 shows the 2D-PAGE separation of proteins of a plasma-membrane-enriched fraction prepared from MDCK II cells after a 2-h chase followed by illumination. Two main radioactive bands at molecular mass and pI similar to those of CAV1, 21- and 24-kDa integral membrane proteins were detected; these radioactive proteins were immunoprecipitated by the anti-CAV1 Ig. Thus the data suggest that the CAV1 proteins are cross-linked to GM3.

A large part of radioactive and photoactivated GM3 was found associated with the detergent-insoluble membrane fraction prepared from fibroblast cells, but a part of the radioactivity was also found associated with the heavier fractions (Fig. 3B, bar 1). As determined in the cell homogenate, the detergent-insoluble membrane fraction prepared from fibroblast cells subjected to 2-h chase contained a much higher level of radioactive CAV1 cross-linked to GM3 than that

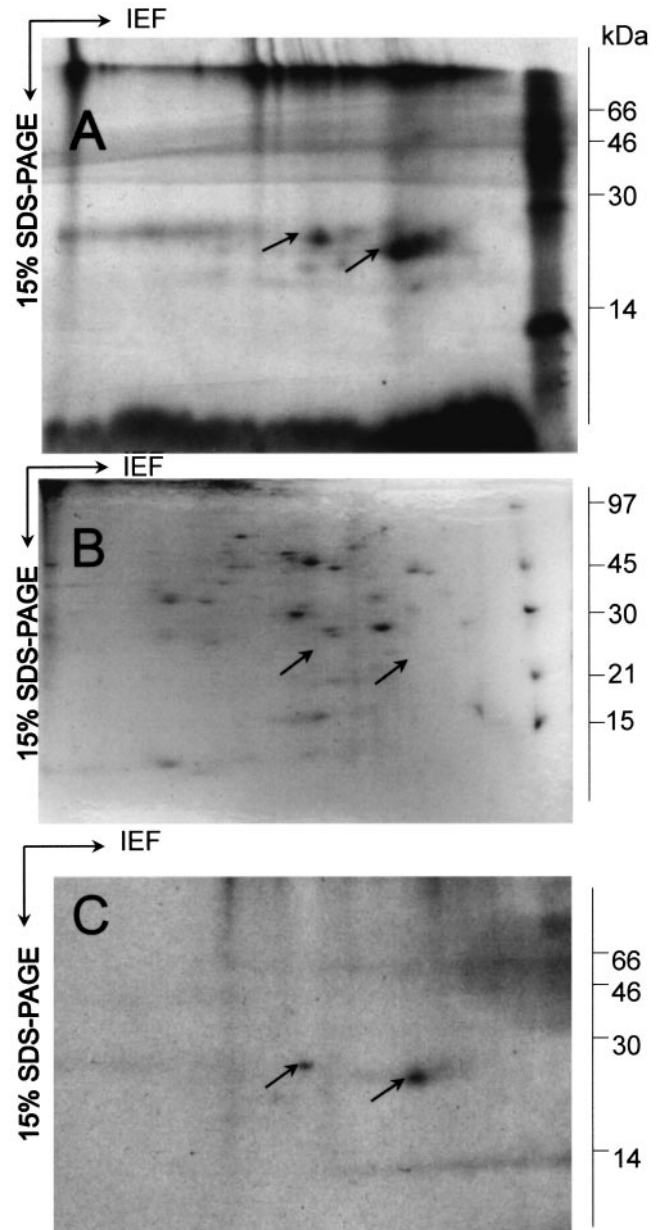
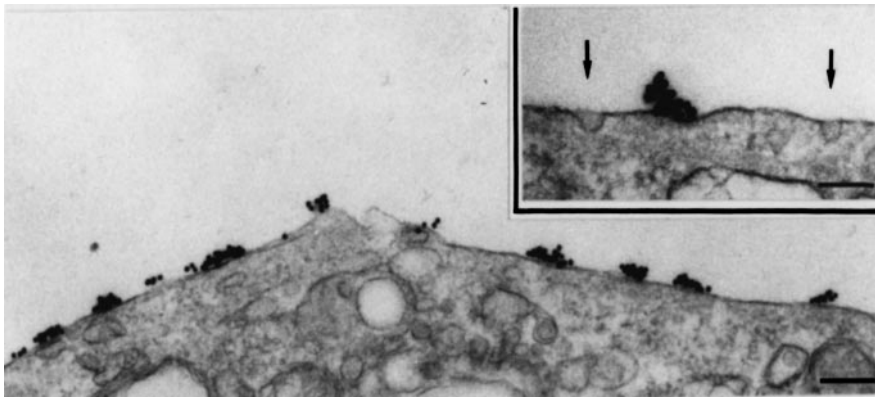


Fig. 7. 2D PAGE of the plasma-membrane-enriched fraction from MDCK II cells subjected to 2-h chase with  $[11\text{-}^3\text{H}(\text{Neu5Ac})]\text{GM3-N}_3$ . (A) Radioactive compounds; arrows indicate the two main radioactive proteins; detection by radioactivity imaging; acquisition time 48 h. (B) Cell protein composition; arrows indicate the pI and mass value of the radioactive bands indicated in (A) (the cell content of caveolin is very low and the protein cannot be colorimetrically stained; detection by Coomassie blue staining). (C), radioactive proteins immunoprecipitated with anti-CAV1 Ig; arrows indicate the two main radioactive proteins that have the same pI and mass value of those indicated in (A); detection by radioactivity imaging; acquisition time 48 h.



**Fig. 8.** Electron microscopy of MDCK II cells after treatment with anti-GM3 Ig and colloidal gold-conjugated protein A. Bar indicates 0.2  $\mu\text{m}$ ; bar in the inset indicates 0.13  $\mu\text{m}$ .

prepared from cells subjected to a 24-h chase (Fig. 4, lanes 5 and 6).

Photolabeling experiments were carried out using the mixture of  $[11\text{-}^3\text{H}(\text{Neu5Ac})]\text{GM3-N}_3/\text{natural GM3}$  (the dilution of the photoactivable derivative with the natural ganglioside is necessary to reduce self quencing during illumination) at a concentration of  $2.5 \times 10^{-5}$  M. Reducing the  $[11\text{-}^3\text{H}(\text{Neu5Ac})]\text{GM3-N}_3/\text{natural GM3}$  concentration to  $5 \times 10^{-6}$  M led to a reduced cell association of radioactivity but did not change the time-dependent process of GM3 cross-linking to CAV1 (data not shown).

### Experiments with $[11\text{-}^3\text{H}(\text{Neu5Ac})]\text{GM3}$

Feeding with  $[11\text{-}^3\text{H}(\text{Neu5Ac})]\text{GM3}$  was performed on cells to establish the radioactivity content of proteins by recycling of sialic acid [38]. This is a control experiment necessary to compare the radioactivity associated with proteins from recycling of sialic acid to that from cross-linking with GM3 after photolabeling experiments with  $[11\text{-}^3\text{H}(\text{Neu5Ac})]\text{GM3-N}_3$ . The radioactivity associated with cell proteins in cells fed  $[11\text{-}^3\text{H}(\text{Neu5Ac})]\text{GM3}$  and subjected to 2- and 24-h chases was about 1 and 19% of the total cell-associated radioactivity, respectively. SDS/PAGE of cells subjected to a 24-h chase shows that mainly high molecular mass radioactive proteins were labeled (Fig. 5). Radioactive proteins with molecular mass in the range of 15–30 kDa were not detected. Similar results were obtained following the recycling of sialic acid in an experiment performed with  $[11\text{-}^3\text{H}(\text{Neu5Ac})]\text{GM3-N}_3$  carried out under dark conditions to avoid transformation of the azide group into nitrene and the following cross-linking processes (data not shown). The radioactivity associated with high molecular mass proteins in

cells fed  $[11\text{-}^3\text{H}(\text{Neu5Ac})]\text{GM3-N}_3$ , subjected to 24-h chase and illuminated, was about 28% of the total cell-associated radioactivity. Thus, from the data on the recycling of radioactive sialic acid, we calculated that about 30% of the high molecular mass radioactive proteins detected in the 24-h chase photolabeling experiment were radioactive by cross-linking with GM3 and about 70% by recycling of the  $[11\text{-}^3\text{H}(\text{Neu5Ac})]\text{GM3-N}_3$  radioactive sialic acid.

The largest part of radioactive GM3 was found associated with the detergent-insoluble membrane fraction prepared from fibroblast cells (Fig. 3B, bar 2).

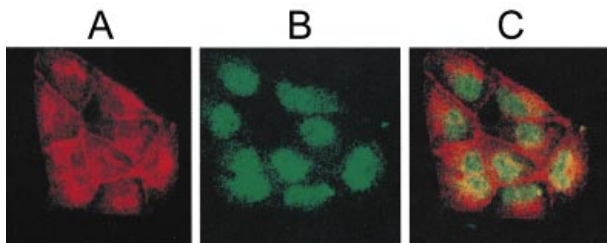
### Microscopy experiments

Figure 8 shows the distribution of ganglioside GM3 in the plasma membranes of MDCK II cells. The figure shows, as revealed by immunoelectron microscopic analysis, an uneven distribution of GM3 in the plasma membrane. The gold immunolabeling, seen as 18-nm dark spherical particles, appeared as clusters over the cell plasma membranes. Control experiments were performed by fixation with glutaraldehyde after the addition of the anti-GM3 mAb and before the addition of the second antibody in order to avoid the possibility that the clustered distribution might result from cross-linking by secondary antibody of only partially immobilized ganglioside molecules. The GM3 clusters were seen close to caveolae structures (arrows in the insert), but no GM3 could be detected in caveolae. Figure 9 shows the scanning confocal microscopy of MDCK II cells after anti-CAV1 and anti-GM3 immunolabeling. Cells appear to be stained in red by anti-CAV1 and in green by anti-GM3. By overlapping the two images and analysing the resulting colors only a very small proportion of the image was colored in yellow, the result of the addition of red with green, i.e. of GM3 and CAV1. This means that colocalization of GM3 and CAV1 in caveolae does not occur, or occurs to a very small extent.

Thus, the microscopy study suggests that in if GM3 is present in caveolae, it occurs at very low levels.

### DISCUSSION

It has been reported [27,39,40] that caveolae and caveolae-like domains of some cells contain gangliosides and that the membrane surface occupied by these domains is enriched, with respect to the remaining membrane surface, in some gangliosides, suggesting that caveolae could be part of sphingolipid domains or one of the sphingolipid domains. Ganglioside GM1 was found to be component of the caveolae in A-431 cells [39] and GM1, but not GD1a, was found in the caveolae-like



**Fig. 9.** Scanning confocal microscopy of MDCK II cells after coimmunostaining with anti-GM3 and anti-CAV1 Ig. Anti-GM3 was stained with FITC-conjugated goat anti-mouse (green fluorophore) and anti-CAV1 with Texas Red-conjugated goat anti-rabbit (red fluorophore) Ig. (A) Texas Red image; (B) FITC image; (C) FITC/Texas Red overlay.



domains in polarized epithelial cells [40], by microscopical studies. Other reports [27] suggest that gangliosides administered to cells for a short time enter cells, becoming components of caveolae of both MDCK II and A-431 cells. More recently, a detergent-insoluble, ganglioside-enriched membrane fraction prepared from tumor cells was further fractionated into two fractions, one enriched in CAV1 and cholesterol, with a low content of sphingomyelin and lacking GM3, the other enriched in sphingolipids [28].

In this study, by combining biochemical and microscopical experiments, we show data that suggest that in cultured MDCK II and fibroblast cells, caveolae and ganglioside GM3-enriched domains are two distinct domains, both present in a detergent-insoluble membrane fraction [4]. Moreover, due to the fact that GM3 is the main cell ganglioside (see also below), caveolae at most contain gangliosides in low quantities.

Fibroblast cells were fed isotopically radiolabeled sphingosine and photoactivable radioactive GM3, and then subjected to the preparation of a detergent-insoluble membrane fraction that is known to be enriched in sphingolipids [4] and caveolae [28].

The metabolic labeling of cells with radioactive sphingosine confirmed that sphingolipids are segregated in membrane microdomains. In fact, the larger part of the metabolically radiolabeled sphingolipids in the cell was found in the detergent-insoluble membrane fraction (Fig. 3).

Experiments with the radioactive and photoactivable GM3 were carried out with the aim to detect proteins present in the ganglioside environment. In previous papers, we treated MDCK II [27] and fibroblast cells [23] with a photoactivable GM1 derivative. By a short pulse–chase experiment, a 21- to 24-kDa membrane protein was cross-linked by the GM1 derivative in both cell lines. This protein was demonstrated to be CAV1 in MDCK II cells. This suggested that GM1 was mainly located in caveolae; however, as GM1 is a minor component of both MDCK II and fibroblast cells, ganglioside GM3 was chosen for these studies because it is the main ganglioside in MDCK II cells (over 90%) [41], and in the human fibroblast line (about 70%) [31]. This should more closely mimic in the behavior of the endogenous gangliosides in these cells. Moreover, we now prolonged the pulse–chase time up to 28 h (4-h pulse followed by 24-h chase).

A large proportion of both radioactive and photoactivated GM3, independent of the chase time, was found associated with the detergent-insoluble membrane fraction, where CAV1 (the characteristic protein of caveolae) was found cross-linked to radioactive GM3 derivative. However, following an extension of the chase time from 2 to 24 h, only trace amounts of radioactive CAV1 protein could be observed. Thus, the cross-linking of GM3 to CAV1 can be considered a transient process.

After a 24-h chase, a large part of GM3 derivative is still at the plasma membrane, as confirmed by the very high cross-linking to membrane lipids (see Fig. 4). This is in agreement with previous data suggesting that the half-life of gangliosides in fibroblasts is about 2–3 days [31,42]. The cross-linking between GM3 and CAV1 is determined by the location of the ganglioside in the caveolae, thus the low level of radiolabeling of the CAV1 after 24-h chase could be determined by: (a) the passage of the GM3 derivative from the caveolae to the ganglioside domains, where the majority of gangliosides are located; and (b) a rapid turnover of caveolae that contain only a minor part of GM3 derivative; our data do not allow to distinguish between the two processes. Nevertheless, they suggest that the GM3 derivative probably enters caveolae in an nonspecific way, and that after ganglioside feeding, some time

is necessary to have the final cell membrane ganglioside organization. Thus, our data suggest that ganglioside GM3 domains and caveolae, both present in a detergent-insoluble membrane fraction, are distinct domains and that caveolae contain at most a low amount of gangliosides.

Experiments based on the administration of gangliosides to cells have been used to study the effects exerted by gangliosides on cell membrane proteins or to study ganglioside metabolism, on the basis that gangliosides taken up by the cells are considered to assume the same orientation and organization of endogenous gangliosides [43,44]. Experiments based on the administration to cells of ganglioside derivatives, used as specific probes, require some care and should be performed in combination with other biochemical experiments to validate the results. In fact the behavior of the ganglioside derivative can be different to that of the natural compound. The behavior of radioactive and photoactivable GM3 was quite similar to that of natural GM3 and after cell feeding it was found largely in the sphingolipid membrane fraction (Fig. 3). Nevertheless, a proportion of it was found associated with the heavier membrane fractions, suggesting some differences in the ganglioside–cell interactions. Thus, we performed microscopy experiments to support our hypothesis that GM3 ganglioside domains and caveolae are separate domains.

Ganglioside domains were detected on the plasma membrane by electron microscopy (Fig. 8), and these domains were well separated from caveolae, where we did not find gold-immunostained gangliosides. Of course, care is necessary in interpreting this result. In fact, if the quantity of gangliosides in caveolae is too low, it is possible that the anti-GM3 Ig cannot bind GM3. The scanning confocal microscopy (Fig. 9) suggests a low level of CAV1 and GM3 colocalization; note that the resolution of this kind of image is not high enough confirm this.

Previous investigations [43,44] have led to the concept that gangliosides enter the plasma membrane as monomers. A specific role of proteins in mediating the uptake process by the cell plasma membranes was never demonstrated. On the other hand, CAV1 is unlikely to mediate the entry of gangliosides into the cell plasma membranes because it is a component of the plasma membrane inner layer [5]. Therefore, we consider that gangliosides administered to cells enter the cell plasma membranes largely by interacting with CAV1, i.e. with caveolae, but with time and in a large enough amount they reach the membrane sphingolipid domains that do not contain caveolae.

Glycosphingolipids are amphiphilic compounds characterized by a very large hydrophilic head group, the oligosaccharide chain. Therefore, from the geometric point of view a large surface area is necessary to accept the glycosphingolipid monomer at the water/lipid interface of the membrane [9]. According to this, a domain enriched in gangliosides will display a membrane geometry characterized by a partially convex curvature [45]. Thus the flask-shaped invagination of caveolae is not an ideal shape for containing endogenous gangliosides or accepting exogenous gangliosides. Of course, this geometric difficulty could be overcome by energy consumption. The portions of caveolae that could be considered ideal for gangliosides could be the edges of invagination, where membrane domains with convex curvatures are also available. Although we do not have direct data, we could also consider the possibility that a cell-mediated increase of the membrane gangliosides can mediate the formation of the caveolae, for example by beginning the formation of the edges of the flask-shaped invagination.

## ACKNOWLEDGEMENTS

This research was supported by the 'Cofinanziamento MURST 1997' to S. S., 'Cofinanziamento MURST 1997' to G. T., 'Cofinanziamento MURST 1998' to V. C.) and by CNR (Grant 97.01225.PF49.115.25597 to S. S.).

## REFERENCES

- Thompson, T.E. & Tillack, T.W. (1985) Organization of glycosphingolipids in bilayers and plasma membranes of mammalian cells. *Annu. Rev. Biophys. Biophys. Chem.* **14**, 361–386.
- Brown, D. & Rose, J.K. (1992) Sorting of GPI-anchored proteins to glycolipid-enriched membrane subdomains during transport to the apical cell surface. *Cell* **68**, 533–544.
- Smart, E.J., Ying, Y.-S., Mineo, C. & Anderson, R.G. (1995) A detergent-free method for purifying caveolae membrane from tissue culture cells. *Proc. Natl Acad. Sci. USA* **92**, 10104–10108.
- Prinetti, A., Iwabuchi, K. & Hakomori, S. (1999) Glycosphingolipid-enriched signaling domain in mouse neuroblastoma Neuro2a cells. Mechanism of ganglioside-dependent neuritogenesis. *J. Biol. Chem.* **274**, 20916–20924.
- Parton, R.G. & Simons, K. (1995) Digging into caveolae. *Science* **269**, 1398–1399.
- Lisanti, M.P., Scherer, P.E., Tang, Z. & Sargiacomo, M. (1994) Caveolae, caveolin and caveolin rich membrane domains: a signaling hypothesis. *Trends Cell Biol.* **4**, 231–235.
- De Pinto, V., Benz, R. & Palmieri, F. (1989) Interaction of non-classical detergents with the mitochondrial porin. A new purification procedure and characterization of the pore-forming unit. *Eur. J. Biochem.* **183**, 179–187.
- Sonnino, S., Cantù, L., Corti, M., Acquotti, D. & Venerando, B. (1994) Aggregative properties of gangliosides in solution. *Chem. Phys. Lipids* **71**, 21–45.
- Cantù, L., Corti, M., Sonnino, S. & Tettamanti, G. (1990) Evidence for spontaneous segregation phenomena in mixed micelles of gangliosides. *Chem. Phys. Lipids* **55**, 223–229.
- Pascher, I. (1976) Molecular arrangements in sphingolipids. Conformation and hydrogen bonding of ceramide and their implication on membrane stability and permeability. *Biochim. Biophys. Acta* **455**, 433–451.
- Ferraretto, A., Pitto, M., Palestini, P. & Masserini, M. (1997) Lipid domains in the membrane: thermotropic properties of sphingomyelin vesicles containing GM1 ganglioside and cholesterol. *Biochemistry* **36**, 9232–9236.
- Ledeer, R.W., Hakomori, S.-I., Yates, A. & Schneider, J.S. & Yu, R.K., ed. (1998) *Ann. N.Y. Acad. Sci.* **845**, 1–433.
- Yamamura, S., Handa, K. & Hakomori, S. (1997) A close association of GM3 with c-Src and Rho in GM3-enriched microdomains at the B16 melanoma cell surface membrane: a preliminary note. *Biochem. Biophys. Res. Commun.* **236**, 218–222.
- Iwabuchi, K., Yamamura, S., Prinetti, A., Handa, K. & Hakomori, S. (1998) GM3-enriched microdomain involved in cell adhesion and signal transduction through carbohydrate-carbohydrate interaction in mouse melanoma B16 cells. *J. Biol. Chem.* **273**, 9130–9138.
- Kasahara, K., Watanabe, Y., Yamamoto, T. & Sanai, Y. (1997) Association of Src family tyrosine kinase Lyn with ganglioside GD3 in rat brain. Possible regulation of Lyn by glycosphingolipid in caveolae-like domains. *J. Biol. Chem.* **272**, 29947–29953.
- Hakomori, S., Handa, K., Iwabuchi, K., Yamamura, S. & Prinetti, A. (1998) New insights in glycosphingolipid function: 'glycosignaling domain', a cell surface assembly of glycosphingolipids with signal transducer molecules, involved in cell adhesion coupled with signaling. *Glycobiology* **8**, 9–18.
- Severs, N.J. (1988) Caveolae: static in-pocketings of the plasma membrane, dynamic vesicles or plain artifact? *J. Cell Sci.* **90**, 341–348.
- Lisanti, M.P., Scherer, P.E., Vidugiriene, J., Tang, Z., Hermanowski-Vosatka, A., Tu, Y.H., Cook, R.F. & Sargiacomo, M. (1994) Characterization of caveolin-rich membrane domains isolated from an endothelial-rich source: implications for human disease. *J. Cell Biol.* **126**, 111–126.
- Mauri, L., Casellato, R., Kirschner, G. & Sonnino, S. (1999) A procedure for the preparation of GM3 ganglioside from GM1-lactone. *Glycoconjugate J.* **16**, 197–203.
- Carter, H.E., Rothfus, J.A. & Gigg, R. (1961) Biochemistry of the sphingolipids: XII. conversion of cerebrosides to ceramides and sphingosine; structure of Gaucher cerebroside. *J. Lipid Res.* **2**, 228–234.
- Sonnino, S., Nicolini, M. & Chigorno, V. (1996) Preparation of radiolabeled gangliosides. *Glycobiology* **6**, 479–487.
- Sonnino, S., Cantù, L., Acquotti, D., Corti, M. & Tettamanti, G. (1990) Aggregation properties of GM3 ganglioside (II3 Neu5AcLacCer) in aqueous solutions. *Chem. Phys. Lipids* **52**, 231–241.
- Sonnino, S., Chigorno, V., Acquotti, D., Pitto, M., Kirschner, G. & Tettamanti, G. (1989) A photoreactive derivative of radio-labeled GM1 ganglioside: preparation and use to establish the involvement of specific proteins in GM1 uptake by human fibroblasts in culture. *Biochemistry* **28**, 77–84.
- Toyokuni, T., Nisar, M., Dean, B. & Hakomori, S.-I. (1991) A facile and regiospecific titration of sphingosine: synthesis of (2S,3R,4E)-2-amino-4-octadecene-1,3-diol-1-<sup>3</sup>H. *J. Labelled Compd. Rad.* **29**, 567–574.
- Dupree, P., Parton, R.G., Raposo, G., Kurzchalia, T.V. & Simons, K. (1993) Caveolae and sorting in the *trans*-Golgi network of epithelial cells. *EMBO J.* **12**, 1597–1605.
- Leroy, J.G., Ho, W.M., McBrinn, M.C., Zielke, K., Jacob, J. & O'Brien, J.S. (1972) I-cell disease: biochemical studies. *Pediatr. Res.* **6**, 752–757.
- Fra, M.A., Masserini, M., Palestini, P., Sonnino, S. & Simons, K. (1995) A photo-reactive derivative of ganglioside GM1 specifically cross-links VIP21-caveolin on the celol surface. *FEBS Lett.* **375**, 11–14.
- Iwabuchi, K., Handa, K. & Hakomori, S.-I. (1998) Separation of 'glycosphingolipid signaling domain' from caveolin-containing membrane fraction in mouse melanoma B16 cells and its role in cell adhesion coupled with signaling. *J. Biol. Chem.* **273**, 33766–33773.
- Tettamanti, G., Bonali, F., Marchesini, S. & Zambotti, V. (1973) A new procedure for the extraction, purification and fractionation of brain gangliosides. *Biochim. Biophys. Acta* **296**, 160–170.
- Taki, T., Handa, S. & Ishikawa, D. (1994) A simple and quantitative purification of glycosphingolipids and phospholipids by thin-layer chromatography blotting. *Anal. Biochem.* **223**, 232–238.
- Chigorno, V., Riva, C., Valsecchi, M., Nicolini, M., Brocca, P. & Sonnino, S. (1997) Metabolic processing of gangliosides by human fibroblasts in culture. Formation and re-cycling of separate pools of sphingosine. *Eur. J. Biochem.* **250**, 661–669.
- Matsudaira, P. (1987) Sequence from picomole quantities of proteins electroblotted onto polyvinylidene difluoride membranes. *J. Biol. Chem.* **262**, 10035–10038.
- Sorice, M., Parolini, I., Sansolini, T., Garofalo, T., Dolo, V., Sargiacomo, M., Tai, T., Peschle, C., Torrisi, M.R. & Pavan, A. (1997) Evidence for the existence of ganglioside-enriched plasma membrane domains in human peripheral lymphocytes. *J. Lipid Res.* **38**, 969–980.
- Brocca, P., Berthault, P. & Sonnino, S. (1998) Conformation of the oligosaccharide chain of GM1 ganglioside in a carbohydrate enriched surface. *Biophys. J.* **74**, 309–318.
- Lowry, O.H., Rosebrough, N.J., Farr, A.L. & Randall, R.J. (1951) Protein measurement with the Folin phenol reagent. *J. Biol. Chem.* **193**, 265–275.
- Riboni, L., Bassi, R., Prinetti, A., Viani, P. & Tettamanti, G. (1999) Predominance of the acylation route in the metabolic processing of exogenous sphingosine in neural and extraneural cells in culture. *Biochem. J.* **338**, 147–151.
- Chigorno, V., Pitto, M., Cardace, G., Acquotti, D., Kirschner, G., Sonnino, S., Ghidoni, R., Tettamanti, G., Association of gangliosides

- to fibroblasts in culture: a & Study performed with, G.M., (1985)  $1^{14}\text{C}$ -labelled at the sialic acid acetyl group. *Glycoconjugate J.* **2**, 279–291.
38. Chigorno, V., Tettamanti, G. & Sonnino, S. (1996) Metabolic processing of gangliosides by normal and Salla cultured human fibroblasts in culture: a study performed by administering radioactive GM3 ganglioside. *J. Biol. Chem.* **271**, 21738–21744.
39. Parton, R.G. (1994) Ultrastructural localization of gangliosides; GM1 is concentrated in caveolae. *J. Histochem. Cytochem.* **42**, 155–166.
40. Wolf, A.A., Jobling, M.G., Wimer-Mackin, S., Ferguson-Maltzman, M., Madara, J.L., Holmes, R.K. & Lencer, W.I. (1998) Ganglioside structure dictates signal transduction by cholera toxin and association with caveolae-like membrane domains in polarized epithelia. *J. Cell Biol.* **141**, 917–927.
41. Nichols, G.E., Shiraishi, T. & Young, W.W. Jr (1988) Polarity of neutral glycolipids, gangliosides, and sulfated lipids in MDCK epithelial cells. *J. Lipid Res.* **29**, 1205–1213.
42. Dawson, G., Matalon, R. & Dorfman, A. (1972) Glycosphingolipids in cultured human skin fibroblasts. I. Characterization and metabolism in normal fibroblasts. *J. Biol. Chem.* **247**, 5944–5950.
43. Kanda, S., Inoue, K., Nojima, S., Utsumi, S. & Wiegandt, H. (1982) Incorporation of a ganglioside and spin-labeled ganglioside analogue into cell and liposomal membranes. *J. Biochem.* **91**, 2095–2098.
44. Schwarzmann, G., Hoffman-Bleilhauer, P., Shubert, J., Sandhoff, K. & Marsh, D. (1983) Incorporation of ganglioside analogues into fibroblast cell membranes. A spin-label study. *Biochemistry* **22**, 5041–5048.
45. Brocca, P. & Sonnino, S. (1997) Dynamic and spatial organization of surface gangliosides. *Trends Glycosci. Glycotechnol.* **9**, 433–445.